The Astrophysical Journal, 788:110 (7pp), 2014 June 20 doi:10.1088/0004-637X/788/2/110

EXTREMELY ORGANIC-RICH COMA OF COMET C/2010 G2 (HILL) DURING ITS OUTBURST IN 2012

Hideyo Kawakita[1], Neil Dello Russo[2], Ron Vervack, Jr.[2], Hitomi Kobayashi[1], Mike A. DiSanti[3], Cyrielle Opitom[4], Emmanuel Jehin[4], Harold A. Weaver[2], Anita L. Cochran[5], Walter M. Harris[6], Dominique Bockelée-Morvan[7], Nicolas Biver[7], Jacques Crovisier[7], Adam J. McKay[8], Jean Manfroid[4], and Michael Gillon[4]
[1] Koyama Astronomical Observatory, Kyoto Sangyo University, Motoyama, Kamitamo, Kita, Kyoto 603-8555, Japan; kawakthd@cc.kyoto-su.ac.jp
[2] The Johns Hopkins University Applied Physics Laboratory, Laurel, MD 20723-6099, USA
[3] Goddard Center for Astrobiology, NASA Goddard Space Flight Center, Greenbelt, MD 20771, USA
[4] F. R. S.–FNRS, Institut d'Astrophysique et de Géophysique, Université de Liège, Allée du 6 août 17, B-4000 Liège, Belgium
[5] McDonald Observatory, 1 University Station C1402, Austin, TX 78712-0259, USA
[6] Department of Applied Sciences, University of California, One Shields Avenue, Davis, CA 95616, USA
[7] LESIA, Observatoire de Paris, CNRS, UPMC, Université Paris-Diderot, 5 Place Jules Janssen, F-92195 Meudon, France
[8] New Mexico State University, Las Cruces, NM 88001, USA
Received 2014 January 8; accepted 2014 April 14; published 2014 May 29

ABSTRACT

We performed high-dispersion near-infrared spectroscopic observations of comet C/2010 G2 (Hill) at 2.5 AU from the Sun using NIRSPEC ($R \approx 25{,}000$) at the Keck II Telescope on UT 2012 January 9 and 10, about a week after an outburst had occurred. Over the two nights of our observations, prominent emission lines of CH_4 and C_2H_6, along with weaker emission lines of H_2O, HCN, CH_3OH, and CO were detected. The gas production rate of CO was comparable to that of H_2O during the outburst. The mixing ratios of CO, HCN, CH_4, C_2H_6, and CH_3OH with respect to H_2O were higher than those for normal comets by a factor of five or more. The enrichment of CO and CH_4 in comet Hill suggests that the sublimation of these hypervolatiles sustained the outburst of the comet. Some fraction of water in the inner coma might exist as icy grains that were likely ejected from nucleus by the sublimation of hypervolatiles. Mixing ratios of volatiles in comet Hill are indicative of the interstellar heritage without significant alteration in the solar nebula.

Key words: comets: general – comets: individual (C/2010 G2 (Hill) – ISM: molecules – protoplanetary disks

Online-only material: color figures

1. INTRODUCTION

There are multiple possible mechanisms for cometary outbursts, but their causes in individual comets are poorly understood. From the viewpoint of observations, a cometary outburst could be defined as the unexpected short-term brightening (increased gas and dust productivity) of a comet. Typically, comet brightness increases rapidly and declines slowly with a decay time of a few weeks. The amplitude of recorded outbursts generally ranges from a few to more than 10 mag. One of the extreme cases was the mega-outburst ($\Delta m \approx 15$ mag in the V band) of comet 17P/Holmes in 2007 at 2.4 AU from the Sun (Santana 2007).

Several mechanisms have been proposed for cometary outbursts. In general, an outburst may be triggered by (1) the interaction of nucleus ices with solar radiation or (2) exothermic processes within the cometary nucleus. In the former case, the solar radiation would cause the sublimation of ices exposed on the surface. Exposure of fresh surface ice could be caused by surface erosion, impacts with other small bodies, or by the fragmentations of the nucleus (caused by the tidal or rotational breakup of the nucleus, etc., as reviewed by Boenhardt 2004). In some cases, the fragmentation might be the result of the buildup of gas pressure in the interior, which is closely related to the outburst described below. Alternatively, the heat wave might propagate from the surface to vaporize highly volatile ices (e.g., very enriched in CO and/or CH_4) within the interior of the nucleus (Whitney 1955). Explosive chemical reactions involving free radicals or unstable molecules might also trigger outbursts (Donn & Urey 1956).

Energy input by solar radiation might also trigger exothermic processes that could result in an outburst. The highly exothermic phase transition of H_2O ice from amorphous to crystalline phases would lead to the rapid release of volatiles trapped in ice (Larson et al. 1990). The exoergic phase transition could provide a significant internal heat source, resulting in the explosive release of gas, ice, and dust grains (Prialnik & Bar-nun 1990). The evaporation of ice grains in the coma also results in an abrupt increase of gas production. Strongly exothermic HCN polymerization might also trigger the sublimation of ices and may contribute to the pressure buildup in the interior of a comet (Rettig et al. 1992). Radioactive decay is another potential heat source for triggering an outburst (Prialnik & Podolak 1999). It is likely that multiple mechanisms are necessary to explain the variety of outbursts that have occurred with different intensities and over a wide range in heliocentric distances.

In this paper, we report the observations of parent volatiles in the coma of comet C/2010 G2 (Hill) roughly one week after its outburst in 2012 January. Comet C/2010 G2 (Hill, hereafter comet Hill) was discovered on 2010 April 10 (Hill 2010). Its high orbital inclination to the ecliptic ($103\overset{\circ}{.}8$) and its Tisserand parameter with respect to Jupiter ($T_J = -0.358 < 2$) suggest an Oort Cloud origin. The perihelion passage was on 2011 September 2 with a perihelion distance of 1.98 AU. The first outburst was detected in late 2010 August with an amplitude of $\Delta m \approx 2$ mag in the optical at around 4.5 AU from the Sun. The second outburst was observed in 2012 January at around 2.5 AU from the Sun after its perihelion passage. The second outburst started about 7–10 days prior to the observations reported here (sometime between 2011 December 30 and 2012 January 2), with an amplitude of $\Delta m \approx 2$ mag in the optical (based on the reports about the nucleus magnitude of comet Hill in MPC 77556–77558 and MPC 77883–77888). No fragments associated with the outburst were detected. Our observations

Table 1
Observational Circumstances for the Near-infrared Observations of C/2010 G2 (Hill)

Date (UT 2012)	Heliocentric Distance, r_h (AU)	Geocentric Distance, Δ (AU)	Relative Velocity to Observer (km s^{-1})	Net Integration Time on Source (minutes)	Grating Settings[a]
January 09.2	2.50	1.94	+41.5	44	KL2
January 09.3	2.50	1.94	+41.5	44	KL1
January 10.2	2.51	1.97	+41.9	18	MW
January 10.3	2.51	1.97	+41.9	64	KL3

Notes. [a] KL1: KL filter with Echelle = 63.75/X-disp = 32.13. KL2: KL filter with Echelle = 62.69/X-disp = 32.06. KL3: KL filter with Echelle = 61.92/X-disp = 32.02. MW: *M*-Wide filter with Echelle = 60.75/X-disp = 35.73. To check wavenumbers covered by each grating setting, the "NIRSPEC Echelle Format Simulator" is available (https://www2.keck.hawaii.edu/inst/nirspec/EFS.html).

and analysis reveal the chemical composition of the cometary ices closely related to the outburst, and the observations could provide a clue to the mechanism of the cometary outburst in C/2010 G2 (Hill).

2. OBSERVATIONS

We performed high-dispersion spectroscopic observations of comet Hill in the *L* band by using the NIRSPEC spectrometer on the Keck II Telescope atop Mauna Kea, Hawaii (McLean et al. 1998) on UT 2012 January 9 and 10. Our observations were carried out about 7–10 days after the beginning of the outburst when the comet productivity was still above its quiescent state but receding. The slit size was $0\farcs432 \times 24''$ corresponding to spectral resolving power of 25,000 for the observations. We used the widest slit ($0\farcs72 \times 24''$) for the observations of a flux standard star (BS718) to maximize the stellar flux through the slit. During spectral integrations, we nodded the telescope $12''$ between the "A" and "B" positions on the $24''$ long slit in a sequence of four scans in the pattern "ABBA." This allows proper cancelation of the sky background emission by performing the operation "A" – "B" – "B" + "A" on the resulting frames. In the case of *L*-band observations of the comet, the net integration time for each ("A" or "B") frame was 60 s (240 s total for each ABBA sequence), while the net integration time for each frame was 10 s (totaling 40 s for each sequence) in the case of the standard star. For *M*-band observations, the net integration time for each frame was 30 s (120 s total for each ABBA sequence) for the comet while the net integration time for each frame was 5 s (20 s total for each sequence) in the case of the standard star. The observational circumstances are summarized in Table 1.

We detected a strong signal from CH_4 emission lines on both nights. On the first night, we also detected strong C_2H_6 emissions along with weak emissions due to H_2O, HCN, and CH_3OH. On the second night, CH_4, HCN, and CO emission lines were also detected in the spectra, but no clear emission lines of H_2O were detected. Figure 1 shows the gallery of the emission spectra of comet Hill obtained by our observations. While we extracted the comet signal within the aperture of $1\farcs68 \times 0\farcs432$ for the *L*-band observations, we used the slightly wider aperture of $2\farcs81 \times 0\farcs432$ for the *M*-band observations. This wider aperture was used because the tracking accuracy of the comet in the *M* band was slightly worse than the *L*-band observations, and the lack of clear continuum and molecular emission within individual spectral differences prevented precise registration of spectral frames in the *M* band. For all settings, the continuum emission (reflected sunlight by the cometary grains) was very weak compared with the emission lines of CH_4, C_2H_6, and CO.

3. RESULTS

We successfully detected the emission lines of H_2O, CO, CH_4, C_2H_6, HCN, and CH_3OH on UT 2012 January 9 and 10 as shown in Figure 1. We detected multiple strong lines of CH_4 (Figure 1), allowing us to determine the rotational temperature (T_{rot}) of CH_4 in the coma on both nights. We also determined the rotational temperatures for H_2O (January 9) and CO (January 10). For other species on these nights, lines were either too weak or insufficient in number to determine a reliable rotational temperature. In such cases, the rotational temperatures of these molecules are assumed to be basically the same as for CH_4 on the same night. We employed the stationary coma model with a constant expansion velocity to obtain the gas production rates of the molecules. The expansion velocity is assumed to be $0.80\ r_h^{-0.5}$ km s^{-1} at r_h AU from the Sun. The photodissociation lifetimes of the molecules are obtained from Huebner et al. (1992) with a dependence of r_h^2. The *g* factors of H_2O (Kawakita & Kobayashi 2009), CH_4 (Kawakita & Kobayashi 2009), and C_2H_6 (Villanueva et al. 2011) were calculated based on the solar fluorescence pumping; the empirical *g* factors of CH_3OH (DiSanti et al. 2013) were recently determined. The rotational temperatures of CH_4 were determined based on the least χ^2 fit of the fluorescence model to the data.

The flux was measured for the small aperture centered at the nucleus as described in the previous section. The gas production rate derived from the small aperture was denoted as the "nucleus-centered gas production rate." Production rates determined from nucleus-centered extracts are generally underestimated due to the effects of guiding errors and seeing, so we did a *Q*-curve analysis to determine the growth factor (GF). This GF is multiplied by the nucleus-centered gas production rate to obtain the corrected "global gas production rate" (DiSanti & Mumma 2008). For some molecules for which we could not determine the GFs due to low signal-to-noise ratios, we assumed the GF of the molecules to be the same as those for CH_4 or C_2H_6 observed at the same time. The flux measurements for each line and their *g* factors are listed in Table 2. The gas production rates of the molecules with the related rotational temperatures and GFs are listed in Table 3.

4. DISCUSSION

Based on our observations, the production rate of $Q(CH_4)$ decreased by ~30% from UT 2012 January 9 to 10. This

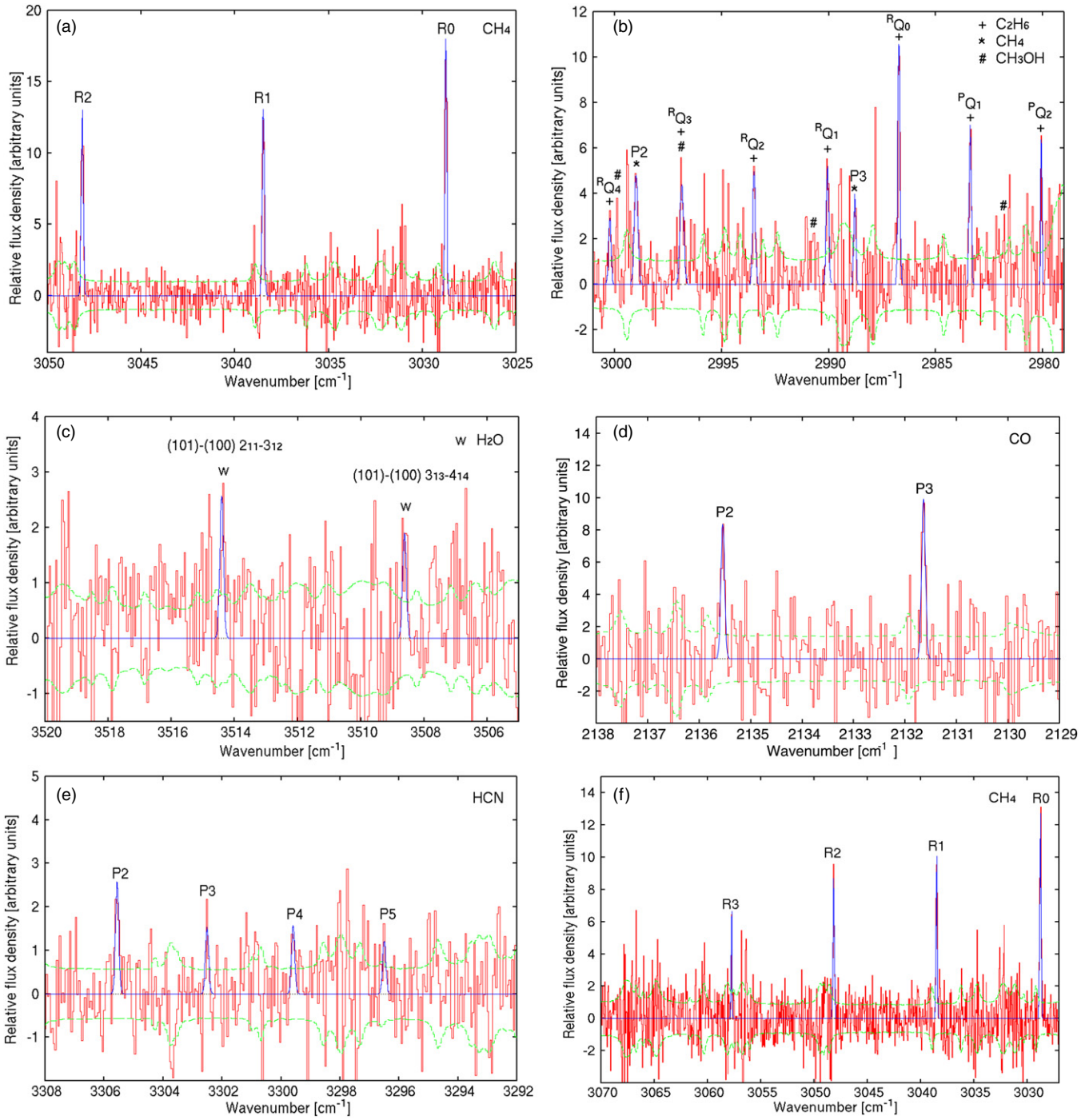

Figure 1. Panels (a)–(c) show the examples of emission spectra taken on January 9 by using KL1 and KL2 settings, and panels (d)–(f) show the examples taken on January 10 by using MW and KL3 settings. Dashed lines are $\pm 1\sigma$ error levels.

(A color version of this figure is available in the online journal.)

suggests that our observations were performed in the fading phase of the outburst. Optical observations also suggest comet Hill was in the fading phase on those dates (MPC 77556–77558, 77883–77888; C. Opitom et al. 2014, in preparation). The rotational temperature of CH_4 may have decreased during these observations, but it is not conclusive (the T_{rot} of CH_4 were consistent within their uncertainties).

We determined the mixing ratios of CH_4, HCN, C_2H_6, and CH_3OH with respect to H_2O based on the near-infrared observations on January 9. Unfortunately, we could not detect H_2O emission lines on January 10. Therefore, we assumed that the CH_4/H_2O ratio did not change between January 9 and 10 to estimate the mixing ratios of CO/H_2O and HCN/H_2O in the comet. Since the mixing ratios of HCN/CH_4 on both dates are consistent with each other within their uncertainties, we consider a constant CH_4/H_2O ratio between January 9 and 10 a reasonable assumption. Table 4 summarizes the mixing ratios in comet Hill at 2.5 AU from the Sun along with the mixing ratios of both the "normal" and "organic-rich" comets observed at around 1 AU from the Sun. The mixing ratios of comet

Table 2
Measured Line Flux and g Factors for Lines Detected in C/2012 G2 (Hill)

Molecule	Rest Wavenumber (cm^{-1})	Vibrational and Rotational Line Identification	Flux[a] (10^{-20} W m^{-2})	g Factor[b] × Transmittance (10^{-7} photons s^{-1}) at 2.5 AU	Setting
		UT 2012 January 09			
H_2O	3508.62	(101)–(100) 3_{13}–4_{14}	2.8 ± 0.7	0.502	KL1
H_2O	3514.41	(101)–(100) 2_{11}–3_{12}	3.8 ± 0.8	0.856	KL1
H_2O	3526.53	(101)–(100) 2_{02}–3_{03}	5.7 ± 0.9	1.04	KL1
HCN	3305.50	ν_3 $P2$	2.62 ± 0.61	40.0	KL2
HCN	3302.61	ν_3 $P3$	1.79 ± 0.60	51.1	KL2
HCN	3299.51	ν_3 $P4$	3.55 ± 0.61	52.8	KL2
HCN	3296.50	ν_3 $P5$	3.10 ± 0.69	44.2	KL2
CH_4	3048.15	ν_3 $R2$	17.7 ± 2.2	49.0	KL2
CH_4	3038.49	ν_3 $R1$	18.8 ± 2.0	45.4	KL2
CH_4	3028.75	ν_3 $R0$	21.7 ± 1.8	61.2	KL2
CH_4	2999.00	ν_3 $P2$	10.1 ± 2.5	23.4	KL1
CH_4	2988.78	ν_3 $P3$	4.8 ± 2.5	11.3	KL1
C_2H_6	3000.23	ν_7 $^RQ_4$	4.4 ± 2.0	18.8	KL1
C_2H_6	2993.49	ν_7 $^RQ_2$	7.7 ± 2.0	41.8	KL1
C_2H_6	2990.06	ν_7 $^RQ_1$	7.9 ± 2.6	43.3	KL1
C_2H_6	2986.72	ν_7 $^RQ_0$	13.0 ± 1.8	76.2	KL1
C_2H_6	2983.39	ν_7 $^PQ_1$	8.8 ± 1.8	58.2	KL1
C_2H_6	2980.07	ν_7 $^PQ_2$	5.0 ± 1.5	38.6	KL1
CH_3OH	3001.21–3000.97	Int. #2[c]	2.9 ± 1.0	5.1	KL1
CH_3OH	3000.01–2999.77	Int. #3[c]	3.3 ± 1.1	3.2	KL1
CH_3OH	2990.89–2990.53	Int. #7[c]	5.2 ± 1.3	5.6	KL1
CH_3OH	2981.99–2981.74	Int. #12[c]	3.7 ± 1.4	4.8	KL1
		UT 2012 January 10			
CO	2131.64	$P3$	89.7 ± 9.6	47.4	MW
CO	2135.54	$P2$	75.5 ± 9.9	43.6	MW
CO	2139.45	$P1$	17.0 ± 11.8	18.7	MW
CO	2147.04	$R0$	57.0 ± 10.5	21.8	MW
CO	2150.88	$R1$	92.3 ± 11.2	33.4	MW
CO	2154.61	$R2$	35.2 ± 11.4	33.6	MW
CO	2158.32	$R3$	59.3 ± 11.7	24.1	MW
H_2O	3453.23	(101)–(100) 2_{02}–3_{21} (200)–(100) 1_{10}–2_{21}	<0.71[d]	0.348	KL3
H_2O	3450.30	(200)–(001) 1_{10}–1_{11}	<0.64[d]	0.251	KL3
H_2O	3439.83	(200)–(001) 1_{11}–1_{10}	<0.66[d]	0.150	KL3
HCN	3320.19	ν_3 $R2$	2.29 ± 0.63	42.7	KL3
HCN	3314.38	ν_3 $R0$	1.51 ± 0.74	17.5	KL3
HCN	3305.57	ν_3 $P2$	3.58 ± 0.56	44.3	KL3
HCN	3302.51	ν_3 $P3$	2.13 ± 0.56	55.4	KL3
HCN	3299.59	ν_3 $P4$	2.17 ± 0.58	55.2	KL3
HCN	3296.50	ν_3 $P5$	1.67 ± 0.68	43.4	KL3
CH_4	3057.75	ν_3 $R3$	7.6 ± 2.5	26.4	KL3
CH_4	3048.17	ν_3 $R2$	14.0 ± 2.2	51.2	KL3
CH_4	3038.50	ν_3 $R1$	13.5 ± 1.7	52.2	KL3
CH_4	3028.76	ν_3 $R0$	20.3 ± 2.0	72.4	KL3

Notes.
[a] Measured flux within the aperture of 1.″68 × 0.″432 (2.″81 × 0.″432) in cases of L-band (M-band) observations.
[b] The fluorescence efficiencies are for the rotational excitation temperatures listed in Table 3.
[c] IDs of spectral interval are from DiSanti et al. (2013).
[d] 3σ upper limit.

17P/Holmes in its mega-outburst at 2.4 AU from the Sun are also listed for comparison. The mixing ratios of organic molecules in comet Hill were higher than not only the normal comets (by a factor of 5–10), but also the organic-rich comets and 17P/Holmes.

It is likely that a significant fraction of H_2O was released from the nucleus of comet Hill as icy grains that evaporated outside our small field of view (FOV). If analogous to that observed in comet 103P/Hartley 2 around the *EPOXI* flyby (A'Hearn et al. 2011), grains of water-rich ice were ejected into the coma by the outgassing of highly volatile molecules such as CO_2. The small aperture of the near-infrared observations might not sample the H_2O gas production from all these icy grains. Alternatively, some fraction of water vaporized during the outburst might re-condense again in the interior of the nucleus or beneath the surface. The temperatures of the interior of the nucleus could be colder than the sublimation temperature of H_2O (∼180 K), which is comparable to the blackbody equilibrium temperature

Table 3
Gas Production Rates and Related Quantities in C/2012 G2 (Hill)

Molecule	T_{rot}[a] (K)	Growth Factor[a]	Q (molecules s^{-1})	Remarks
UT 2012 January 9				
CH_4	48^{+9}_{-7}	1.54 ± 0.10	$(5.5 \pm 0.5) \times 10^{26}$	KL2
HCN	(48)	(1.54)	$(7.7 \pm 1.1) \times 10^{25}$	KL2
H_2O	38^{+9}_{-6}	(1.45)	$(6.1 \pm 0.3) \times 10^{27}$	KL1
CH_4	~44[b]	(1.45)	$(6.1 \pm 1.4) \times 10^{26}$	KL1
C_2H_6	(50)	1.45 ± 0.07[c]	$(2.3 \pm 0.3) \times 10^{26}$	KL1
CH_3OH	(50)	(1.45)	$(1.1 \pm 0.2) \times 10^{27}$	KL1
UT 2012 January 10				
CO	34^{+11}_{-7}	2.15 ± 0.14	$(4.7 \pm 0.7) \times 10^{27}$	MW
CH_4	42^{+6}_{-5}	1.51 ± 0.03	$(4.0 \pm 0.3) \times 10^{26}$	KL3
HCN	(42)	(1.51)	$(6.5 \pm 0.8) \times 10^{25}$	KL3
H_2O	(42)	(1.51)	$<7.1 \times 10^{27}$	KL3

Notes.
[a] Numbers in the parentheses are assumed values.
[b] Two lines were detected in this setting, which are too few to estimate reliable error. If we assume $T_{rot} = 48$ K (as was derived in the KL2 setting) for CH_4, $Q(CH_4)$ increases by a few percent only and within the range listed in the table.
[c] Determined from the continuum emission recorded in the same Echelle order.

at 2.5 AU from the Sun. Therefore, it is possible that a significant fraction of the originally sublimated H_2O did not reach the coma. These possibilities could explain the overabundant highly volatile species in the coma of comet Hill during the outburst. Thus, derived abundances of coma gases may not be indicative of the abundances of volatile ices in the nucleus of comet Hill.

There is no obvious evidence of water sublimation from icy grains in the inner coma based on the spatial distribution of water emissions because the water emissions in our spectra were too weak to obtain spatial profiles. However, we note that infrared observations of comet 17P/Holmes revealed no clear evidence of water sublimation from icy grains within our aperture, even with robust water spatial profiles (Dello Russo et al. 2008). Imaging observations at optical wavelengths were performed by the 60 cm TRAPPIST (Jehin et al. 2011) robotic telescope with an OH narrowband filter on UT 2012 January 9.05 by (C. Opitom et al. 2014, in preparation). The estimated gas production rate is $Q(OH) = (1.3 \pm 0.2) \times 10^{28}$ molecules s^{-1}, assuming typical scale lengths and outgassing velocities of parent and daughter species (1 km s^{-1}). Assuming a branching ratio of 0.85, $Q(H_2O) \sim 1.5 \times 10^{28}$ molecules s^{-1}, which is higher than $Q(H_2O)$ obtained in our near-infrared observations on January 9 by a factor of ~2.5. This is not surprising as the $22' \times 22'$ FOV of the optical imaging observations can sample water sublimated outside the much smaller FOV of the infrared observations. However, we should note that the photodissociation lifetime of H_2O at 2.5 AU is about six days. The Q(OH) obtained on January 9 reflected the water gas production rates in the earlier phase of the outburst, which was considered to be larger than $Q(H_2O)$ on January 9. Thus, the water gas production rate estimated from Q(OH) on January 9 is very likely overestimated and should be considered as an upper limit. While the existence of icy grains in the inner coma on January 9 is highly suggestive, it is not conclusive from these observations.

Because some fraction of water might exist as icy grains or not fully sublimated from the nucleus, we focus on the abundance ratios among highly volatile species (except H_2O) in Table 4. Of course, icy grains (if present) might also contain other highly volatile species. Similar spatial distributions between H_2O and CH_3OH in comet 103P/Hartley 2 (Mumma et al. 2011; Dello Russo et al. 2011; Kawakita et al. 2013) were indicative of the coexistence of H_2O and CH_3OH. We have to keep in mind that some fraction of CH_3OH (or other volatiles) might exist in icy grains in the case of comet Hill. Figure 2 shows the relative mixing ratios compared to the "normal" comets. Even though we consider the upper limit for water gas production rate (including the potential contribution from icy grains), the mixing ratios of comet Hill during the outburst are higher than the "normal" comets, even those extremely enriched in organics. The significant enrichment of CO suggests the outburst was fueled by its release. Another hypervolatile, CO_2, might also be important for the outburst because the *Akari* survey for $CO_2/CO/H_2O$ in 18 comets (Ootsubo et al. 2012) revealed that, even in this relatively small sample, a substantial number of comets contain abundant CO_2 ice. However, there is no information about the gas production rate of CO_2 in comet Hill. The rapid sublimation of CO (and/or other hypervolatiles) at 2.5 AU from the Sun could be triggered by the energy input, for example, of the phase change from amorphous to crystalline water ices. However, based on our observations, we cannot identify the energy source(s) for outburst in the case of comet Hill.

Table 4
Comparison of Volatile Mixing Ratios in Comets and Interstellar Ices

	Comet Hill	Organic Normal[a]	Organic Rich[b]	17P/Holmes at 2.4 AU in Outburst[c]	Interstellar Ices Toward Low-mass Proto-stars[d]	T_{sub}[e] (K)
H_2O	100	100	100	100	100	180
CO	107 ± 23	4.0	3.9	~4	20–61	25
CH_4[f]	9.0 ± 0.9	1.0	1.2	...	4–7	31
C_2H_6	3.8 ± 0.4	0.6	1.7	1.8 ± 0.3	...	44
HCN	1.3 ± 0.2	0.25	0.1–0.6	0.54 ± 0.08	0.2–0.8[g]	95
CH_3OH	18 ± 3	2.0	3.0	4.1 ± 0.6	5–12	99

Notes.
[a] Gibb et al. (2012).
[b] Magee-Sauer et al. (2008).
[c] Dello Russo et al. (2008) for the molecules except CO. We assume $CO/CH_3OH \sim 1$ based on Biver et al. (2008) to estimate CO/H_2O.
[d] Öberg et al. (2011).
[e] Meech & Svoren (2004).
[f] We assumed the CH_4/H_2O ratio is unchanged between January 9 and 10.
[g] X-CN ices.

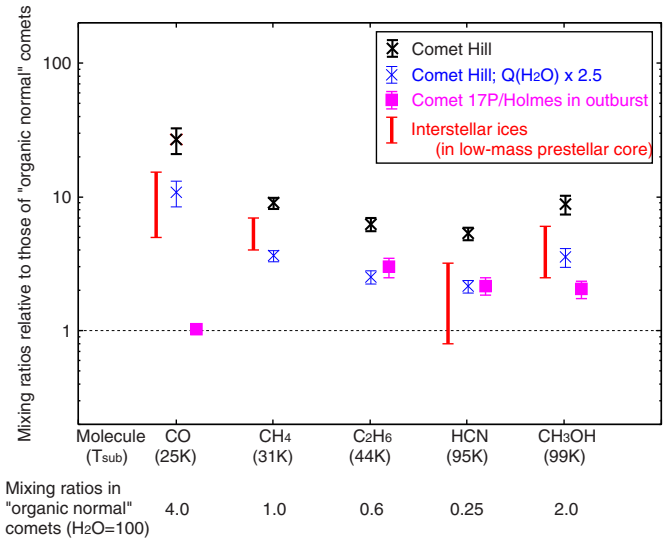

Figure 2. Mixing ratios of comet Hill (with and without potential contribution of missing water vapor; see the text) relative to those of the organic "normal" comets. The relative mixing ratios of comet 17P/Holmes and interstellar ices are also shown for comparison.

(A color version of this figure is available in the online journal.)

The pattern of molecular abundances (except H_2O) in comet Hill is clearly different from the "normal" comet as shown in Figure 2. However, we note that the mixing ratios for "normal" comets were derived from the observations at around 1 AU from the Sun, where most volatile ices completely evaporate. In the case of observations at 2.5 AU from the Sun, less volatile ices might not fully sublimate from the nucleus. Therefore, even for a "normal comet," the relative composition derived from the coma observations at 2.5 AU may be enriched in hypervolatiles such as CO and CH_4 ($T_{sub} \sim 30$ K) with respect to moderately volatile ices such as HCN and CH_3OH ($T_{sub} \sim 100$ K). Although there are no reports on high-dispersion near-infrared spectra of a comet in modest outburst at around 2.5 AU from the Sun, there are a few reports for bright comets not in outburst at ~2.5 AU. In comet C/1995 (Hale-Bopp), Dello Russo et al. (2000, 2001) reported the gas production rates of C_2H_6 and H_2O at 2.24 AU, and the resultant C_2H_6/H_2O ratio is $>0.43\% \pm 0.11\%$. In comet C/2009 P1 (Garradd), Paganini et al. (2012) reported $C_2H_6/H_2O > 2.9\%$ at 2.40 AU from the Sun. It is clear that a larger sample size is needed, and it is possible that if more data were available on "normal comets" in non-outburst conditions at 2.5 AU, abundances in Hill at 2.5 AU might not be atypical. However, for a detailed comparison, we have to wait for more appearances of bright comets, even at large heliocentric distances, or wait for the next-generation telescopes with larger apertures (e.g., Thirty Meter Telescope with the 30 m aperture).

A comparison between comets Hill and 17P/Holmes during outburst is also interesting. Although the outbursts occurred at similar heliocentric distances, the molecular mixing ratios of those comets are different from each other. The differences in volatile abundances may indicate different mechanisms for outburst in different comets (indeed, the magnitudes of the outbursts are quite different between comets Hill and 17P/Holmes). As listed in Table 4, the mixing ratios of C_2H_6, HCN, and CH_3OH are similar in these comets. However, the mixing ratio of CO is smaller in comet 17P/Holmes (Biver et al. 2008) than in comet Hill. On the other hand, Capria et al. (2010) reported the ratio of the green (557.7 nm) to red lines (630.0 and 636.4 nm) of atomic oxygen to be 0.1 ± 0.11 in 17P/Holmes one day after the outburst started. This ratio of ~0.1 indicates that the H_2O molecule was the main parent of the forbidden oxygen emission lines, while higher line ratios suggest that more CO_2 is present rather than H_2O (Cochran et al. 2008; McKay et al. 2012, 2013; Decock et al. 2013). Therefore, CO_2 might play a less important role than H_2O in the case of the outburst of 17P/Holmes.

Finally, we note that the mixing ratios in comet Hill are similar to those of the interstellar ices in the low-mass prestellar environments (Öberg et al. 2011), as shown in Figure 2. Although a fraction of H_2O might be missed in the near-infrared observations with small apertures (i.e., some fraction of water existed as ice grains in the coma or H_2O did not fully sublimate from the nucleus due to relatively lower temperatures of the nucleus) and therefore the mixing ratios of volatile species with respect to H_2O in the nucleus are somewhat overestimated compared to actual values, the relative ratios among CO, CH_4, HCN, and CH_3OH in comet Hill are indeed similar to those of interstellar ices. Of course, this should be re-examined in future (after obtaining new results for comets observed at ~2.5 AU) because at present there are few comparisons with our comet Hill results. At present, we propose the hypothesis that the nucleus of comet Hill contained a significant amount of interstellar ices that were largely unaltered by physical and chemical processes in the solar nebula. The ices enriched in hypervolatiles might trigger and sustain the outburst phenomena of comet Hill.

This work was supported by a NASA Keck PI Data Award administered by the NASA Exoplanet Science Institute. Data presented here were obtained at the W. M. Keck Observatory from telescope time allocated to the National Aeronautics and Space Administration through the agency's scientific partnership with the California Institute of Technology and the University of California. The observatory was made possible by the generous financial support of the W. M. Keck Foundation. The authors recognize and acknowledge the very significant cultural role and reverence that the summit of Mauna Kea has always had within the indigenous Hawaiian community. We are most fortunate to have the opportunity to conduct observations from this mountain. This work was also financially supported by MEXT under Grant-in-Aid for Scientific Research 22540257 (H. Kawakita).

REFERENCES

A'Hearn, M. F., Belton, M. J. S., Delamere, W. A., et al. 2011, Sci, 332, 1396
Biver, N., Bockelée-Morvan, D., Wiesemeyer, H., et al. 2008, LPICo, 1405, 8146
Boenhardt, H. 2004, in Comet II, ed. M. C. Festou, H. U. Keller, & H. A. Weaver (Tucson, AZ: Univ. Arizona Press), 301
Capria, M. T., Cremonese, G., & de Sanctis, M. C. 2010, A&A, 522, A82
Cochran, A. L. 2008, Icar, 198, 181
Decock, A., Jehin, E., Hutsemékers, D., & Manfroid, J. 2013, A&A, 555, A34
Dello Russo, N., Mumma, M. J., DiSanti, M. A., Magee-Sauer, K., & Novak, R. 2001, Icar, 153, 162
Dello Russo, N., Mumma, M. J., DiSanti, M. A., et al. 2000, Icar, 143, 324
Dello Russo, N., Vervack, R. J., Jr., Lisse, C. M., et al. 2011, ApJL, 734, L8
Dello Russo, N., Vervack, R. J., Jr., Weaver, H. A., et al. 2008, ApJ, 680, 793
DiSanti, M. A., Bonev, B. P., Villanueva, G. L., & Mumma, M. J. 2013, ApJ, 763, 1
DiSanti, M. A., & Mumma, M. J. 2008, SSRv, 138, 127
Donn, B., & Urey, H. C. 1956, ApJ, 123, 339
Gibb, E. L., Bonev, B. P., Villanueva, G. L., et al. 2012, ApJ, 750, 102
Hill, R. E. 2010, IAUC, 9134, 1
Huebner, W. F., Keady, J. J., & Lyon, S. P. 1992, Ap&SS, 195, 1
Jehin, E., Gillon, M., Queloz, D., et al. 2011, Msngr, 145, 2
Kawakita, H., & Kobayashi, H. 2009, ApJ, 693, 388
Kawakita, H., Kobayashi, H., Dello Russo, N., et al. 2013, Icar, 222, 723

Larson, H. P., Hu, H-Y., Mumma, M. J., & Weaver, H. A. 1990, Icar, 86, 129
Magee-Sauer, K., Mumma, M. J., DiSanti, M. A., et al. 2008, Icar, 194, 347
McKay, A. J., Chanover, N. J., Morgenthaler, J. P., et al. 2012, Icar, 220, 277
McKay, A. J., Chanover, N. J., Morgenthaler, J. P., et al. 2013, Icar, 222, 684
McLean, I. S., Becklin, E. E., Bendiksen, O., et al. 1998, Proc. SPIE, 3354, 566
Meech, K. J., & Svoren, J. 2004, in Comet II, ed. M. C. Festou, H. U. Keller, & H. A. Weaver (Tucson, AZ: Univ. Arizona Press), 317
Mumma, M. J., Bonev, B. P., Villanueva, G. L., et al. 2011, ApJL, 734, L7
Öberg, K. I., Boogert, A. C. A., Pontoppidan, K. M., et al. 2011, ApJ, 740, 109
Ootsubo, T., Kawakita, H., Hamada, S., et al. 2012, ApJ, 752, 15
Paganini, L., Mumma, M. J., Villanueva, G. L., et al. 2012, ApJL, 748, L13
Prialnik, D., & Bar-nun, A. 1990, ApJ, 363, 274
Prialnik, D., & Podolak, M. 1999, SSRv, 90, 169
Rettig, T. W., Tegler, S. C., Pasto, D. J., & Mumma, M. J. 1992, ApJ, 398, 293
Santana, J. A. H. 2007, IAUC, 8886, 1
Villanueva, G. L., Mumma, M. J., & Magee-Sauer, K. 2011, JGR, 116, E08012
Whitney, C. 1955, ApJ, 122, 190